

## Templated Synthesis of the Novel Layered Silver–Antimony Sulfides $[\text{H}_3\text{NCH}_2\text{CH}_2\text{NH}_2][\text{Ag}_2\text{SbS}_3]$ and $[\text{H}_3\text{NCH}_2\text{CH}_2\text{NH}_2]_2[\text{Ag}_5\text{Sb}_3\text{S}_8]$

Paz Vaquero,<sup>†</sup> Ann M. Chippindale,<sup>‡</sup> Andrew R. Cowley,<sup>§</sup> and Anthony V. Powell<sup>\*,†</sup>

Department of Chemistry, Heriot-Watt University, Edinburgh EH14 4AS, United Kingdom, School of Chemistry, The University of Reading, Whiteknights, Reading RG6 6AD, United Kingdom, and Chemical Crystallography Laboratory, University of Oxford, Oxford, OX1 3PD, United Kingdom

Received August 4, 2003

Two new silver–antimony sulfides,  $[\text{C}_2\text{H}_9\text{N}_2][\text{Ag}_2\text{SbS}_3]$  (**1**) and  $[\text{C}_2\text{H}_9\text{N}_2]_2[\text{Ag}_5\text{Sb}_3\text{S}_8]$  (**2**), have been prepared solvothermally in the presence of ethylenediamine and characterized by single-crystal X-ray diffraction, thermogravimetry, and elemental analysis. Compound **1** crystallizes in the space group *Pn* ( $a = 6.1781(1) \text{ \AA}$ ,  $b = 11.9491(3) \text{ \AA}$ ,  $c = 6.9239(2) \text{ \AA}$ ,  $\beta = 111.164(1)^\circ$ ) and **2** in the space group *Pm* ( $a = 6.2215(2) \text{ \AA}$ ,  $b = 15.7707(7) \text{ \AA}$ ,  $c = 11.6478(5) \text{ \AA}$ ,  $\beta = 92.645(2)^\circ$ ). The structure of **1** consists of chains of fused five-membered  $\text{Ag}_2\text{SbS}_2$  rings linked to form layers, between which the template molecules reside. Compound **2** contains honeycomb-like sheets of fused silver–antimony–sulfide six-membered rings linked to form double layers. The idealized structure can be considered to be an ordered defect derivative of that of lithium bismuthide,  $\text{Li}_3\text{Bi}$ , and represents a new solid-state structure type.

### Introduction

Templated synthesis, in which reactions are performed under solvothermal conditions in the presence of a structure-directing agent such as an organic amine, has proved to be a versatile route for the fabrication of novel oxygen-based frameworks.<sup>1</sup> Following the report<sup>2</sup> that template-directed synthesis can be applied to effect the crystallization of tin and germanium sulfides, there has been considerable interest in the solvothermal synthesis of chalcogenides. The majority of materials produced to date contain the main-group elements arsenic, antimony, tin, indium, and germanium. The structural features of these materials have been recently reviewed.<sup>3,4</sup>

Introduction of transition-metal ions into solvothermal reactions involving antimony sulfide generally results in the

formation of an anionic antimony–sulfide framework together with a charge-balancing cationic transition-metal complex, as exemplified by  $[\text{M}(\text{en})_3][\text{Sb}_2\text{S}_4]$  ( $\text{M} = \text{Co}, \text{Ni}$ ) and  $[\text{M}(\text{en})_3][\text{Sb}_4\text{S}_7]$  ( $\text{M} = \text{Fe}, \text{Ni}$ ).<sup>5</sup> There have been comparatively few reports of the incorporation of transition metals into main-group metal sulfide frameworks by means of solvothermal synthesis.<sup>6–8</sup> The coinage metals appear to be more readily incorporated into the primary antimony–sulfide bonding network than the early-transition-series elements. For example, the synthesis of anionic copper–antimony–sulfide frameworks, in which  $\text{Cu}_8\text{S}_{13}$  cores are linked by antimony atoms to form channels that contain transition-metal hexamine cations, has been reported.<sup>9</sup> The mixed-valent Cu(I)/Cu(II) sulfide  $[\text{C}_2\text{H}_8\text{N}_2]_{0.5}[\text{Cu}_2\text{SbS}_3]^{10}$  and the isostructural selenide,<sup>11</sup> together with the copper sulfide  $[\text{C}_4\text{H}_{12}\text{N}_2]_{0.5}[\text{CuSb}_6\text{S}_{10}]^{12}$  in which pairs of edge-sharing

\* Author to whom correspondence should be addressed. Fax: +44 (0)-131 451 3180. E-mail: a.v.powell@hw.ac.uk.

<sup>†</sup> Heriot-Watt University.

<sup>‡</sup> The University of Reading.

<sup>§</sup> University of Oxford.

(1) Cheetham, A. K.; Férey, G.; Loiseau, T. *Angew. Chem., Int. Ed.* **1999**, *38*, 3268.

(2) Bedard, R. L.; Wilson, S. T.; Vail, L. D.; Bennett, J. M.; Flanigen, E. M. In *Zeolites: Facts, Figures, Future*; Jacobs, P., van Santen, R. A., Eds.; Elsevier: Amsterdam, 1989.

(3) Sheldrick, W. S. *J. Chem. Soc., Dalton Trans.* **2000**, 3041.

(4) Li, J.; Chen, Z.; Wang, R. J.; Proserpio, D. M. *Coord. Chem. Rev.* **1999**, *190–192*, 707.

(5) Stephan, H. O.; Kanatzidis, M. G. *Inorg. Chem.* **1997**, *36*, 6050.

(6) Stephan, H. O.; Kanatzidis, M. G. *J. Am. Chem. Soc.* **1996**, *118*, 12226.

(7) Engelke, L.; Schaefer, M.; Schur, M.; Bensch, W. *Chem. Mater.* **2001**, *13*, 1383.

(8) Kiebach, R.; Bensch, W.; Hoffmann, R.-D.; Pöttgen, R. *Z. Anorg. Allg. Chem.* **2003**, *629*, 532.

(9) Schimek, G. L.; Kolis, J. W.; Long, G. J. *Chem. Mater.* **1997**, *9*, 2776.

(10) Powell, A. V.; Boissière, S.; Chippindale, A. M. *J. Chem. Soc., Dalton Trans.* **2000**, 4192.

(11) Chen, Z.; Dilks, R. E.; Wang, R.; Lu, J. Y.; Li, J. *Chem. Mater.* **1998**, *10*, 3184.

(12) Powell, A. V.; Paniagua, R.; Vaquero, P.; Chippindale, A. M. *Chem. Mater.* **2002**, *14*, 1220.

$\text{CuS}_4$  distorted tetrahedra form pillars between  $\text{Sb}_6\text{S}_{10}^{2-}$  layers, have also recently been described.

The heavier congener, silver, has also been incorporated into antimony–sulfide frameworks by reactions in supercritical ammonia. A range of three-dimensional anionic frameworks including  $\text{MAg}_2\text{SbS}_4$  ( $\text{M} = \text{K}, \text{Rb}$ ),  $\text{K}_2\text{AgSbS}_4$ , and the layered material  $\text{Rb}_2\text{AgSbS}_4$  have been prepared.<sup>13</sup> Reactions in the presence of larger cations favor the formation of one-dimensional anionic chains, as found in  $\text{Cs}_3\text{Ag}_2\text{Sb}_3\text{S}_8$ ,  $\text{Cs}_2\text{AgSbS}_4$ ,<sup>14</sup> and  $[\text{Fe}(\text{NH}_3)_6][\text{AgSbS}_4]$ .<sup>9</sup> These reactions demonstrate that it is the size and charge of the relatively simple cationic species that principally determine the structures of thioantimonates prepared in supercritical ammonia. However, the synthesis of metal chalcogenides in polyamine solvents suggests that, in contrast to supercritical ammonia, the polyamine plays a templating role and has a marked influence on the structure and dimensionality of the final product. This effect may be a consequence of hydrogen bonding between the template and the host.

Given the enormous potential to generate new structure types using solvothermal methods, we have extended our work on copper–antimony sulfides to silver-containing materials. Here, we describe the first amine-templated silver–antimony sulfides,  $[\text{C}_2\text{H}_9\text{N}_2][\text{Ag}_2\text{SbS}_3]$  (**1**) and  $[\text{C}_2\text{-H}_9\text{N}_2]_2[\text{Ag}_5\text{Sb}_3\text{S}_8]$  (**2**). Both materials consist of complex silver–antimony–sulfide layers, separated by ethylenediamine molecules. The structure of **1** is closely related to those of the copper–antimony chalcogenides  $[\text{C}_2\text{H}_8\text{N}_2]_x[\text{Cu}_2\text{SbQ}_3]$  ( $x = 0.5$ ,  $\text{Q} = \text{S}$ ,<sup>10</sup>  $\text{Se}$ ;<sup>11</sup>  $x = 1.0$ ,  $\text{Q} = \text{Se}$ <sup>11</sup>). However, **2** provides an entirely new structure type related to  $\text{Li}_3\text{Bi}$ , in which simultaneous occupation of half of the tetrahedral and all of the octahedral interstitial sites between pairs of close-packed anion layers is seen for the first time.

## Experimental Section

Initially,  $\text{Sb}_2\text{S}_3$  (0.68 g, 2 mmol),  $\text{AgNO}_3$  (0.34 g, 2 mmol), and **S** (0.16 g, 5 mmol) were loaded into a 23 mL Teflon-lined stainless steel autoclave. Ethylenediamine (5 mL) was added to form a mixture with an approximate molar composition,  $\text{Sb}_2\text{S}_3:\text{AgNO}_3:\text{S}:\text{en} = 2:2:5:75$ . After the mixture was stirred, the container was closed, heated at 180 °C for 14 days, and then cooled to room temperature at a cooling rate of 20 °C  $\text{h}^{-1}$ . The reaction mixture was filtered, washed with ethanol and deionized water, and dried in air at room temperature. Under these conditions, the product consists of a mixture of black blocks, yellow plates of **1** and a very small amount of orange needles of **2**. Powder X-ray diffraction data on a ground portion of the bulk sample were collected with nickel-filtered  $\text{Cu K}\alpha$  radiation ( $\lambda = 1.5418 \text{ \AA}$ ), using a Philips PA2000 powder diffractometer. The diffraction pattern indicates the presence of two phases: the condensed phase pyrrargyrite,  $\text{Ag}_3\text{-SbS}_3$ ,<sup>15</sup> which comprises the black blocks, together with a phase that can be indexed on the basis of the monoclinic unit cell determined from the single-crystal diffraction study of **1**. Owing to the small number of crystals of **2** present, no reflections from

this phase could be identified in the powder diffraction pattern of the bulk sample.

Subsequent synthetic studies were directed at attempts to produce single-phase materials. Samples that contain mainly phase **1** were prepared by heating a mixture with a molar composition  $\text{Sb}_2\text{S}_3:\text{AgNO}_3:\text{S}:\text{en}$  of 0.5:2:5:75, at a temperature of 160 °C for a 7 day period. Large amounts of phase **1** were also found to result from mixtures with  $\text{Sb}_2\text{S}_3:\text{AgNO}_3$  ratios in the range 0.25–0.35 and  $\text{AgNO}_3:\text{S}$  ratios of 0.8–2.5, at temperatures in the range 160–180 °C. Samples containing larger amounts of crystals of **2**, together with some crystals of **1** and dark red/black blocks, subsequently identified by single-crystal X-ray diffraction as the condensed phase  $\text{Ag}_3\text{SbS}_3$ ,<sup>15</sup> were prepared from mixtures with a molar composition  $\text{Sb}_2\text{S}_3:\text{AgNO}_3:\text{S}:\text{en}$  of 1:1:2.5:75 at 190 °C.

The yellow plates of **1** and the orange needles of **2** were separated from bulk samples by handpicking. Combustion analysis for the crystals of **1** gave C, 4.78; H, 1.82; N, 5.14% (calcd for  $[\text{C}_2\text{H}_9\text{N}_2][\text{Ag}_2\text{SbS}_3]$ : C, 4.85; H, 1.82; N, 5.66%), and for **2**, C, 3.66; H, 1.43; N, 4.01% (calcd for  $[\text{C}_2\text{H}_9\text{N}_2]_2[\text{Ag}_5\text{Sb}_3\text{S}_8]$ : C, 3.74; H, 1.40; N, 4.36%). Analytical electron microscopy, performed using a Philips XL30 scanning microscope equipped with an EDAX “Phoenix” detection system, gave Ag:S and Sb:Ag ratios of 0.60-(5) and 0.58(6) for **1** and 0.60(5) and 0.61(4) for **2**. These are in good agreement with the values calculated from the respective crystallographically determined compositions of  $[\text{C}_2\text{H}_9\text{N}_2][\text{Ag}_2\text{SbS}_3]$  and  $[\text{C}_2\text{H}_9\text{N}_2]_2[\text{Ag}_5\text{Sb}_3\text{S}_8]$ .

Thermogravimetric analysis was performed using a DuPont Instruments 951 thermal analyzer. Approximately 8 mg of finely ground crystals of each material was heated under a flow of dry nitrogen over the temperature range 25–290 °C at a heating rate of 2 °C  $\text{min}^{-1}$ . Weight losses of 13.05% for **1** and 9.1% for **2** compare favorably with respective values of 12.3% and 9.5% calculated for the removal of ethylenediamine molecules. Powder X-ray diffraction patterns of the decomposition products indicate that in both cases thermal decomposition produces  $\text{Ag}_3\text{SbS}_3$  and an unidentified minor phase.

**Crystal Structure Determination.** X-ray intensity data for crystals of **1** and **2** were collected at room temperature using a Nonius KappaCCD diffractometer (graphite-monochromated  $\text{Mo K}\alpha$  radiation). Both data sets were processed using DENZO<sup>16</sup> and SCALEPACK.<sup>17</sup> Full crystallographic details are given in Table 1.

The structures were solved by direct methods using the program SIR92<sup>18</sup> and all framework atoms located. Subsequent Fourier calculations and least-squares refinements on  $F$  were carried out using the CRYSTALS suite of programs.<sup>19</sup> Carbon and nitrogen atoms of the template were located in difference Fourier maps. For **1**, the C and N atoms were refined anisotropically and the template H atoms placed geometrically after each cycle of refinement, while for **2** anisotropic thermal parameters were refined for the C atoms only. The N atoms, which were found to be disordered over two crystallographically inequivalent positions, were modeled isotropically and their site occupancies refined. Hydrogen atoms were not included in the refinement. Both crystals were found to be

(13) Schimek, G. L.; Pennington, W. T.; Wood, P. T.; Kolis, J. W. *J. Solid State Chem.* **1996**, *123*, 277.

(14) Wood, P. T.; Schimek, G. L.; Kolis, J. W. *Chem. Mater.* **1996**, *8*, 721.

(15) Harker, D. J. *Chem. Phys.* **1936**, *4*, 381.

(16) Otwinowski, Z. *DENZO*; Department of Molecular Biophysics and Biochemistry, Yale University: New Haven, CT, 1993.

(17) Otwinowski, Z. *SCALEPACK*; Department of Molecular Biophysics and Biochemistry, Yale University: New Haven, CT, 1993.

(18) Altomare, A.; Cascarano, G.; Giacovazzo, C.; Guagliardi, A.; Burla, M. C.; Polidori, G.; Camelli, M. *J. Appl. Crystallogr., Sect. A* **1994**, *27*, 435.

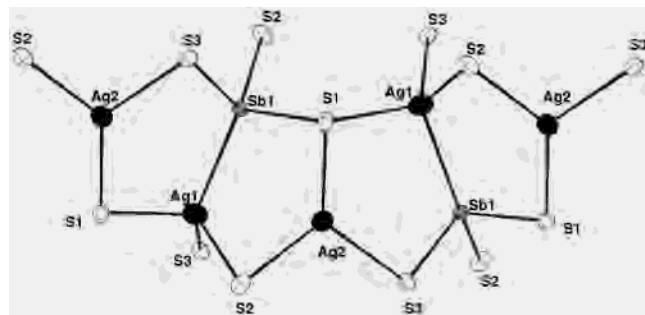
(19) Watkin, D. J.; Prout, C. K.; Carruthers, J. R.; Betteridge, P. W.; Cooper, R. I. *CRYSTALS Issue 11*; Chemical Crystallography Laboratory, University of Oxford: Oxford, U.K., 2001.

**Table 1.** Crystallographic Data for [C<sub>2</sub>H<sub>9</sub>N<sub>2</sub>][Ag<sub>2</sub>SbS<sub>3</sub>] (**1**) and [C<sub>2</sub>H<sub>9</sub>N<sub>2</sub>]<sub>2</sub>[Ag<sub>5</sub>Sb<sub>3</sub>S<sub>8</sub>] (**2**)

	<b>1</b>	<b>2</b>		<b>1</b>	<b>2</b>
<i>M<sub>r</sub></i>	494.82	1265.27	<i>V/Å<sup>3</sup></i>	476.67	1136.88
crystal habit	yellow plate	orange rod	<i>Z</i>	2	2
dimensions/mm	0.01 × 0.24 × 0.3	0.02 × 0.04 × 0.24	wavelength/Å	0.71073	0.71073
crystal system	monoclinic	monoclinic	<i>μ/cm<sup>-1</sup></i>	7.47	8.42
space group	<i>Pn</i>	<i>Pm</i>	no. of measured data	6353	8707
<i>T/K</i>	293(2)	293(2)	no. of unique data	1940	4706
<i>a/Å</i>	6.1781(1)	6.2215(2)	no. of obsd data ( <i>I</i> > 3σ( <i>I</i> ))	1908	3953
<i>b/Å</i>	11.9491(3)	15.7707(7)	<i>R<sub>merge</sub>/%</i>	3.50	3.10
<i>c/Å</i>	6.9239(2)	11.6478(5)	<i>R</i> /%	3.81	3.05
<i>β/deg</i>	111.164(1)	92.645(2)	<i>R<sub>w</sub>/%</i>	4.26	3.15

**Table 2.** Fractional Atomic Coordinates and Equivalent Isotropic Thermal Parameters (Å<sup>2</sup>) for Non-Hydrogen Atoms in **1**

atom	x	y	z	<i>U<sub>iso</sub></i>
Sb(1)	-0.0473(1)	0.39688(3)	0.8723 (1)	0.0157
Ag(1)	-0.1487(1)	0.61728(5)	0.9607(1)	0.0304
Ag(2)	-0.1440(1)	0.39568(5)	0.3645(1)	0.0342
S(1)	0.3247(3)	0.4018(1)	0.8322(3)	0.0225
S(2)	-0.2613(3)	0.2691(2)	0.5980(3)	0.0221
S(3)	0.0419(3)	0.2725(2)	1.1681(2)	0.0196
N(1)	-0.499(1)	0.1639(5)	1.080(1)	0.0288
N(2)	-0.244(1)	-0.1247(5)	1.163(1)	0.0288
C(1)	-0.432(1)	0.0532(6)	1.181(1)	0.0286
C(2)	-0.300(1)	-0.0123(5)	1.0682(9)	0.0221

**Figure 1.** Local coordination of the framework atoms in **1** showing the atom labeling scheme and ellipsoids at 50% probability. Fusion of five-membered silver–antimony–sulfide rings generates [Ag<sub>2</sub>SbS<sub>3</sub>]<sup>-</sup> chains parallel to [1 0 -1].

inversion twins with Flack parameters of 0.43(4) and 0.54(3) for **1** and **2**, respectively.

## Results and Discussion

**Structure of [C<sub>2</sub>H<sub>9</sub>N<sub>2</sub>][Ag<sub>2</sub>SbS<sub>3</sub>] (**1**).** The atomic coordinates and isotropic thermal parameters of non-hydrogen atoms of **1** are given in Table 2. Figure 1 shows the local coordination of the framework atoms, while selected bond lengths and angles are presented in Table 3. In common with other reported antimony sulfides, the antimony atom is trigonal pyramidally coordinated by sulfur (Table 3). However, unusually for this class of material, there are no significant secondary Sb–S interactions at distances within the sum of the van der Waals' radii of Sb and S (3.80 Å).<sup>20</sup>

Both silver atoms are coordinated by three sulfur atoms at distances in the range 2.432(2)–2.646(2) Å, in an approximately trigonal pyramidal coordination for Ag(1) and a nearly trigonal planar coordination for Ag(2). Although silver sulfides commonly exhibit tetrahedral coordination of silver,<sup>21</sup> trigonal pyramidal and trigonal planar coordinations

**Table 3.** Selected Bond Lengths (Å) and Angles (deg) for **1**<sup>a</sup>

Sb(1)–S(1)	2.413(2)	S(1)–Sb(1)–S(2)	101.43(6)
Sb(1)–S(2)	2.424(2)	S(1)–Sb(1)–S(3)	100.16(6)
Sb(1)–S(3)	2.427(2)	S(2)–Sb(1)–S(3)	99.72(6)
Sb(1)–Ag(1)	2.8249(7)	S(1) <sup>a</sup> –Ag(1)–S(3) <sup>c</sup>	121.16(6)
Sb(1)–Ag(2)	3.3467(8)	S(2) <sup>b</sup> –Ag(1)–S(3) <sup>c</sup>	109.93(6)
Ag(1)–S(1) <sup>a</sup>	2.646(2)	S(1) <sup>a</sup> –Ag(1)–S(2) <sup>b</sup>	93.52(6)
Ag(1)–S(2) <sup>b</sup>	2.614(2)	S(1) <sup>c</sup> –Ag(2)–S(3) <sup>d</sup>	124.29(7)
Ag(1)–S(3) <sup>c</sup>	2.589(2)	S(2)–Ag(2)–S(3) <sup>d</sup>	106.73(5)
Ag(1)–Ag(2) <sup>a</sup>	2.891(1)	S(1) <sup>c</sup> –Ag(2)–S(2)	128.93(7)
Ag(2)–S(1) <sup>c</sup>	2.432(2)		
Ag(2)–S(2)	2.505(2)		
Ag(2)–S(3) <sup>d</sup>	2.542(2)		

<sup>a</sup> Symmetry transformations used to generate equivalent atoms: (a) *x* – 1/2, 1 – *y*, *z* + 1/2. (b) *x* + 1/2, 1 – *y*, *z* + 1/2. (c) *x* – 1/2, 1 – *y*, *z* – 1/2. (d) *x*, *y*, *z* – 1.

have been reported in materials such as CsAg<sub>7</sub>S<sub>4</sub>,<sup>22</sup> KAg<sub>5</sub>S<sub>3</sub>,<sup>23</sup> and RbAg<sub>2</sub>As<sub>3</sub>Se<sub>6</sub>,<sup>24</sup> for which Ag–S distances and angles are similar to those determined here. In addition, Ag(1) has a neighboring antimony atom at a distance of 2.8249(7) Å, resulting in a pseudotetrahedral coordination of Sb(1). The Ag(1)–Sb(1) distance is considerably shorter than those found in the condensed phases Ag<sub>3</sub>SbS<sub>3</sub> (3.04 Å)<sup>15</sup> and AgSbS<sub>2</sub> (3.8 Å),<sup>25</sup> and is similar to the Ag–Sb distance in Ag<sub>3</sub>Sb,<sup>26</sup> indicating significant intermetallic bonding. The Ag(1)–Sb(1) bond completes a nearly planar five-membered silver–antimony–sulfide ring. Fusion of these rings along the edges formed by Ag(2)–S(1) and Ag(1)–Sb(1) bonds produces puckered chains directed along [1 0 -1] (Figure 1). Individual chains are connected by Sb(1)–S(2) and Ag(1)–S(3) bonds to form layers parallel to the (001) crystallographic plane (Figure 2). The interchain Ag(1)–Ag(2) separation of 2.891(1) Å is similar to the Ag–Ag distance of 2.88 Å in the elemental structure,<sup>27</sup> and to metal–metal distances in monovalent silver compounds in which there are significant d<sup>10</sup>–d<sup>10</sup> interactions.<sup>28,29</sup>

Ethylenediamine molecules are located between metal–sulfide layers to which they are approximately perpendicularly aligned (Figure 3). The terminal nitrogen atoms are

(20) Bondi, A. J. *J. Phys. Chem.* **1964**, *68*, 441.

(21) Auernhammer, M.; Effenberger, H.; Irran, E.; Pertlik, F.; Rosenstingl, J. *J. Solid State Chem.* **1993**, *106*, 421.

(22) Wood, P. T.; Pennington, W. T.; Kolis, J. W. *Inorg. Chem.* **1994**, *33*, 1556.

(23) Emiridag, M.; Schimek, G. L.; Kolis, J. W. *Acta Crystallogr.* **1998**, *C54*, 1376.

(24) Wachhold, M.; Kanatzidis, M. G. *Inorg. Chem.* **1999**, *38*, 4178.

(25) Knowles, C. R. *Acta Crystallogr.* **1964**, *17*, 847.

(26) Scott, J. D. *Can. Mineral.* **1976**, *14*, 139.

(27) Wells, A. F. *Structural Inorganic Chemistry*, 5th ed.; Clarendon: Oxford, England, 1984.

(28) Jansen, M. *Angew. Chem., Int. Ed. Engl.* **1987**, *26*, 1098.

(29) Cui, C. X.; Kertesz, M. *Inorg. Chem.* **1990**, *29*, 2568.

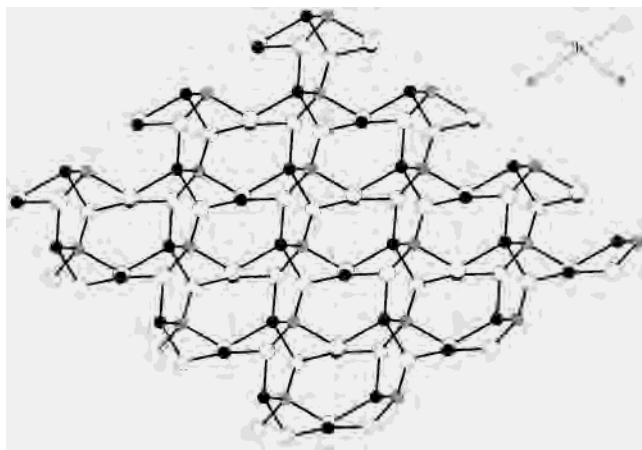


**Figure 2.** View along the [010] direction showing a  $[\text{Ag}_2\text{SbS}_3]^-$  layer formed by linking chains of five-membered rings via Ag(1)–S(3) and Sb–S(2). Key: silver, large black circles; antimony, large shaded circles; sulfur, large open circles.

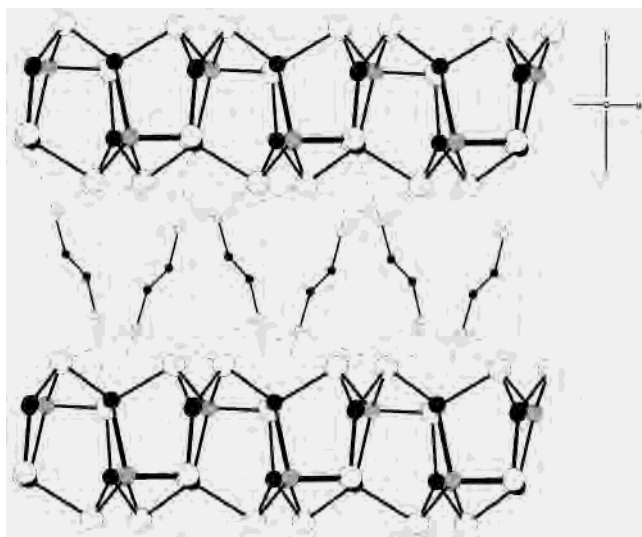


**Figure 3.** View along the [001] direction showing the locations of the monoprotonated ethylenediamine molecules in **1**. Dashed lines correspond to the short sulfur–nitrogen distances and show a possible network of hydrogen bonds. Key: silver, large black circles; antimony, large shaded circles; sulfur, large open circles; carbon, small black circles; nitrogen, small open circles. Hydrogen atoms have been omitted for clarity.

directed at the two neighboring layers, separated by ca. 6 Å. Each nitrogen has four sulfur neighbors at distances in the range 3.29–3.65 Å, implying hydrogen-bonding interactions between the template and the framework.

Although similar heterometallic layers are found in copper–antimony selenides and sulfides, there are differences in the orientation of the ethylenediamine molecules situated between the layers.  $[\text{C}_2\text{H}_8\text{N}_2]_{0.5}[\text{Cu}_2\text{SbSe}_3]^{11}$  and  $[\text{C}_2\text{H}_8\text{N}_2]_{0.5}[\text{Cu}_2\text{SbS}_3]^{10}$  are isostructural and have the ethylenediamine molecules orientated parallel to the layers. In  $[\text{C}_2\text{H}_8\text{N}_2][\text{Cu}_2\text{SbSe}_3]^{11}$  however, the amine molecules are aligned perpendicular to the layers, analogous to the arrangement in  $[\text{C}_2\text{H}_9\text{N}_2][\text{Ag}_2\text{SbS}_3]$  reported here.

The structural study was unable to establish directly the degree of protonation of the template molecules. While magnetic susceptibility and EPR measurements indicate that  $[\text{C}_2\text{H}_8\text{N}_2]_{0.5}[\text{Cu}_2\text{SbSe}_3]$ ,  $[\text{C}_2\text{H}_8\text{N}_2]_{0.5}[\text{Cu}_2\text{SbS}_3]$ , and  $[\text{C}_2\text{H}_8\text{N}_2]$ -

**Table 4.** Fractional Atomic Coordinates and Equivalent Isotropic Thermal Parameters ( $\text{\AA}^2$ ) for Non-Hydrogen Atoms in **2**

atom	<i>x</i>	<i>y</i>	<i>z</i>	$U_{\text{iso}}$	Occ <sup>a</sup>
Sb(1)	−0.3904(2)	0	0.1920 (1)	0.0209	
Sb(2)	−0.0915(2)	0.5	0.5445(1)	0.0197	
Sb(3)	0.1276(2)	0.36390(4)	0.30703(9)	0.0212	
Sb(4)	−0.6078(2)	0.13315(4)	0.42900(9)	0.0222	
Ag(1)	−0.4348(2)	0.5	0.3134(1)	0.0338	
Ag(2)	−0.4311(2)	0.22759(6)	0.2067(1)	0.0450	
Ag(3)	−0.1881(2)	−0.28399(6)	0.5200(1)	0.0441	
Ag(4)	0.0240(2)	0.15061(6)	0.1958(1)	0.0480	
Ag(5)	−0.6641(2)	−0.35274(5)	0.5426(1)	0.0539	
Ag(6)	−0.1215(3)	0	0.3987(2)	0.0550	
S(1)	0.1868(5)	0.5	0.2010(3)	0.0235	
S(2)	−0.4879(5)	0.5	0.5468(3)	0.0242	
S(3)	−0.2616(4)	0.3543(1)	0.3109(2)	0.0236	
S(4)	−0.7756(5)	0	0.1967(3)	0.0296	
S(5)	−0.0080(4)	−0.3811(1)	0.6701(2)	0.0259	
S(6)	−0.8019(4)	0.2879(2)	0.1365(2)	0.0289	
S(7)	0.0039(4)	−0.1485(1)	0.4262(2)	0.0280	
S(8)	−0.5167(4)	0.2108(2)	0.6014(2)	0.0284	
S(9)	−0.5451(6)	0	0.5404(3)	0.0305	
S(10)	−0.3212(4)	0.1175(1)	0.0663(2)	0.0264	
C(1)	0.955(2)	0.1515(8)	0.784(1)	0.0670	
C(2)	1.161(2)	0.1519(9)	0.861(1)	0.0698	
C(3)	0.725(2)	0.3435(8)	0.959(1)	0.0693	
C(4)	0.522(2)	0.3446(8)	0.879(1)	0.0555	
N(10)	0.949(3)	0.083(1)	0.697(1)	0.083(7)	0.79(3)
N(11)	0.813(6)	0.076(2)	0.792(4)	0.04(1)	0.21(3)
N(20)	1.298(3)	0.076(1)	0.842(2)	0.046(8)	0.42(3)
N(21)	1.168(4)	0.077(1)	0.939(2)	0.066(7)	0.58(3)
N(30)	0.864(4)	0.419(1)	0.944(2)	0.053(8)	0.44(3)
N(31)	0.721(5)	0.421(1)	1.031(2)	0.071(8)	0.56(3)
N(40)	0.508(3)	0.417(1)	0.798(1)	0.064(7)	0.63(3)
N(41)	0.384(3)	0.421(1)	0.897(2)	0.043(8)	0.37(3)

<sup>a</sup> The site occupancy factors are 1.00 unless stated otherwise.

$[\text{Cu}_2\text{SbSe}_3]$  contain Cu(I) and Cu(II),<sup>10,11</sup> rendering the layers neutral and hence requiring a non-protonated amine, oxidation states of silver higher than Ag(I) are unlikely to be favored in a chalcogenide matrix. This conclusion is supported by magnetic susceptibility measurements which show the material to be diamagnetic ( $\chi_{\text{mol}} \approx -8 \times 10^{-4}$  emu mol<sup>−1</sup>) at room temperature. Therefore, monovalent silver and trivalent antimony result in anionic  $[\text{Ag}_2\text{SbS}_3]^-$  layers, necessitating monoprotonation of the ethylenediamine molecules and formulation of **1** as  $[\text{C}_2\text{H}_9\text{N}_2][\text{Ag}_2\text{SbS}_3]$ .

**Structure of  $[\text{C}_2\text{H}_9\text{N}_2]_2[\text{Ag}_5\text{Sb}_3\text{S}_8]$  (**2**).** Atomic coordinates and isotropic thermal parameters of non-hydrogen atoms of **2** are presented in Table 4, and the local coordination of the framework atoms is shown in Figure 4. Selected bond lengths and angles are presented in Table 5. Compound **2** crystallizes in a new structure type, consisting of silver–antimony–sulfide double layers separated by ethylenediamine template molecules. Formal valence considerations as above suggest that the  $[\text{Ag}_5\text{Sb}_3\text{S}_8]$  layer is doubly negatively charged. Each antimony atom is approximately trigonal pyramidally coordinated by sulfur (Table 5). In common with the majority of other templated antimony sulfides, there are additional Sb–S interactions at longer distances of 3.54–3.76 Å, less than the sum of the van der Waals' radii of Sb and S.

The silver atoms Ag(1), Ag(3), and Ag(4) exhibit a distorted tetrahedral coordination, with an average Ag–S distance of 2.63 Å, comparable to values in the literature for silver sulfides in tetrahedral coordination.<sup>21</sup> The atoms

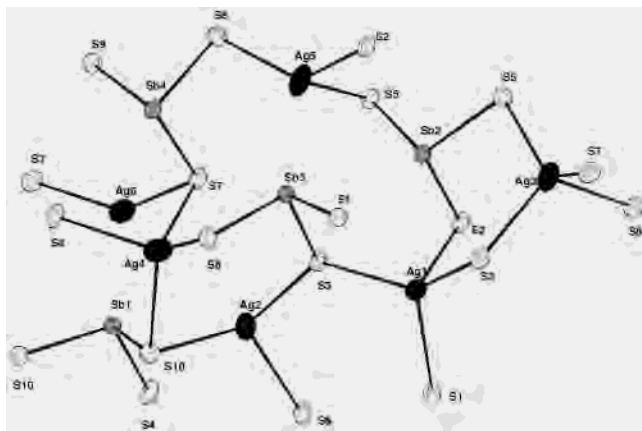


**Figure 4.** Local coordination of the framework atoms in **2** showing the atom labeling scheme and ellipsoids at 50% probability.

**Table 5.** Selected Bond Lengths (Å) and Angles (deg) for **2**<sup>a</sup>

Sb(1)–S(4)	2.399(3)	Ag(3)–S(3) <sup>a</sup>	2.696(3)
Sb(1)–S(10)/S(10) <sup>a</sup>	2.412(2) 2	Ag(3)–S(5)	2.545(2)
Sb(1)–Ag(6)	2.868(2)	Ag(3)–S(7)	2.703(2)
Sb(2)–S(2)	2.468(3)	Ag(3)–S(8) <sup>a</sup>	2.567(2)
Sb(2)–S(5) <sup>a</sup> /S(5) <sup>b</sup>	2.420(2) × 2	Ag(3)–Ag(5)	3.176(1)
Sb(2)–Ag(1)	3.358(1)	Ag(3)–Ag(5) <sup>c</sup>	3.434(1)
Sb(3)–S(1)	2.512(2)	Ag(4)–S(4) <sup>c</sup>	2.682(2)
Sb(3)–S(3)	2.429(2)	Ag(4)–S(6) <sup>c</sup>	2.531(3)
Sb(3)–S(6) <sup>c</sup>	2.378(2)	Ag(4)–S(7) <sup>a</sup>	2.693(3)
Sb(3)–Ag(5) <sup>d</sup>	2.985(1)	Ag(4)–S(10)	2.619(2)
Sb(4)–S(7) <sup>e</sup>	2.427(2)	Ag(4)–Ag(6)	3.499(2)
Sb(4)–S(8)	2.398(3)	Ag(5)–S(2) <sup>h</sup>	2.568(2)
Sb(4)–S(9)	2.490(2)	Ag(5)–S(5) <sup>f</sup>	2.698(3)
Sb(4)–Ag(2)	3.220(1)	Ag(5)–S(8) <sup>a</sup>	2.502(3)
Ag(1)–S(1) <sup>f</sup>	2.640(3)	Ag(6)–S(7)/S(7) <sup>a</sup>	2.485(2) × 2
Ag(1)–S(2)	2.754(4)		
Ag(1)–S(3)/S(3) <sup>g</sup>	2.538(2) × 2		
Ag(2)–S(3)	2.542(2)		
Ag(2)–S(6)	2.592(3)		
Ag(2)–S(10)	2.502(2)		
Ag(2)–Ag(4)	3.089(1)		
S(4)–Sb(1)–S(10)/S(10) <sup>a</sup>	102.74(8) × 2	S(3) <sup>a</sup> –Ag(3)–S(5)	115.07(8)
S(10)–Sb(1)–S(10) <sup>a</sup>	100.4(1)	S(3) <sup>a</sup> –Ag(3)–S(7)	91.13(8)
S(2)–Sb(2)–S(5) <sup>a</sup> /S(5) <sup>b</sup>	100.37(8) × 2	S(5)–Ag(3)–S(7)	124.39(8)
S(5) <sup>a</sup> –Sb(2)–S(5) <sup>b</sup>	101.5(1)	S(3) <sup>a</sup> –Ag(3)–S(8) <sup>a</sup>	114.44(8)
S(1)–Sb(3)–S(3)	103.36(9)	S(5)–Ag(3)–S(8) <sup>a</sup>	110.47(8)
S(1)–Sb(3)–S(6) <sup>c</sup>	89.04(9)	S(7)–Ag(3)–S(8) <sup>a</sup>	99.68(8)
S(3)–Sb(3)–S(6) <sup>c</sup>	101.91(8)	S(4) <sup>c</sup> –Ag(4)–S(6) <sup>c</sup>	123.63(9)
S(7) <sup>e</sup> –Sb(4)–S(8)	99.02(8)	S(4) <sup>c</sup> –Ag(4)–S(7) <sup>a</sup>	91.6(1)
S(7) <sup>e</sup> –Sb(4)–S(9)	102.9(1)	S(6) <sup>c</sup> –Ag(4)–S(7) <sup>a</sup>	108.83(8)
S(8)–Sb(4)–S(9)	88.23(9)	S(4) <sup>c</sup> –Ag(4)–S(10)	101.20(9)
S(1) <sup>f</sup> –Ag(1)–S(2)	110.2(1)	S(6) <sup>c</sup> –Ag(4)–S(10)	111.31(8)
S(1) <sup>f</sup> –Ag(1)–S(3)/S(3) <sup>g</sup>	111.32(6) × 2	S(7) <sup>a</sup> –Ag(4)–S(10)	119.78(8)
S(2)–Ag(1)–S(3) <sup>g</sup>	94.68(7) × 2	S(2) <sup>h</sup> –Ag(5)–S(5) <sup>f</sup>	100.84(9)
S(3)–Ag(1)–S(3)	129.7(1)	S(2) <sup>h</sup> –Ag(5)–S(8) <sup>a</sup>	130.77(9)
S(3)–Ag(2)–S(6)	101.88(8)	S(5) <sup>f</sup> –Ag(5)–S(8) <sup>a</sup>	106.72(8)
S(3)–Ag(2)–S(10)	137.54(8)	S(7)–Ag(6)–S(7) <sup>a</sup>	141.0(1)
S(6)–Ag(2)–S(10)	108.33(8)	S(3) <sup>a</sup> –Ag(3)–S(5)	115.07(8)
S(4)–Sb(1)–S(10)/S(10) <sup>a</sup>	102.74(8) × 2		

<sup>a</sup> Symmetry transformations used to generate equivalent atoms: (a)  $x, -y, z$ . (b)  $x, 1 + y, z$ . (c)  $1 + x, y, z$ . (d)  $1 + x, y, -z$ . (e)  $x - 1, -y, z$ . (f)  $x - 1, y, z$ . (g)  $x, 1 - y, z$ . (h)  $x, y - 1, z$ .

Ag(2) and Ag(5) are trigonal pyramidally coordinated by sulfur, whereas the atom Ag(6) has only two short bonds to S(7) (at 2.485(2) Å), and a weaker interaction with a third sulfur atom, S(9), at a somewhat longer distance of 3.174(4) Å. The short Ag(6)–S(7) distances are slightly longer than those previously reported for two-coordinate silver atoms (2.38–2.41 Å),<sup>22,23</sup> and the S(7)–Ag(6)–S(7) angle of 141.0(1)° deviates significantly from linearity, suggesting

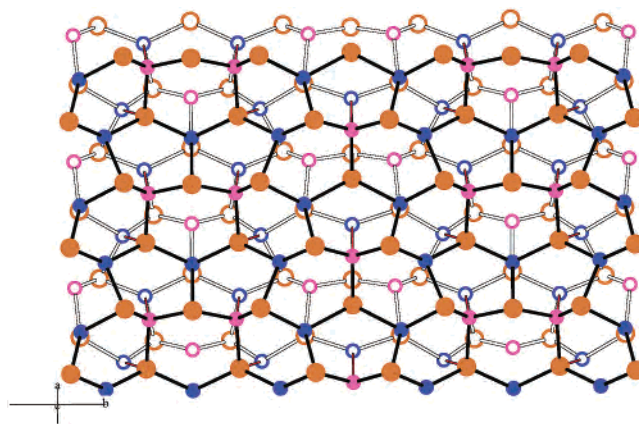


**Figure 5.** View along the [001] direction of a  $[\text{Ag}_5\text{Sb}_3\text{S}_8]^{2-}$  double layer formed from linkage of two crystallographically distinct distorted honeycomb-like sheets. Each sheet is comprised of fused six-membered silver–antimony–sulfide rings. Key: silver, blue circles; antimony, pink circles; sulfur, orange circles. Atoms and bonds in the upper sheet (containing Sb(1), Sb(3), Ag(1), Ag(2), and Ag(4)) are shown as solid circles and lines, while those in the lower sheet (containing Sb(2), Sb(4), Ag(3), Ag(5), and Ag(6)) are drawn as open circles and lines. Intersheet metal–sulfur bonds are marked in red. Metal–metal bonds have been omitted for clarity.

Ag(6) is best described as trigonally coordinated. There are also short contacts between Ag(6) and Sb(1) (2.868(2) Å), and Ag(5) and Sb(3) (2.985(1) Å), with values comparable to those found in silver–antimony alloys,<sup>26</sup> indicating significant intermetallic bonding. The atoms Sb(2) and Sb(4) also have neighboring Ag atoms at relatively short distances of 3.358(1) and 3.224(1) Å, respectively, which are less than the sum of the van der Waals' radii of Sb and Ag (3.70 Å).<sup>20</sup> Vertex-linking of the  $\text{SbS}_3$ ,  $\text{AgS}_4$ , and  $\text{AgS}_3$  units produces six-membered rings, in which metal and nonmetal atoms alternate. Mirror planes at  $(x, 0, z)$  and  $(x, \frac{1}{2}, z)$  generate two distorted honeycomb-like sheets parallel to (001). Within a given sheet, the majority of rings contain one Sb atom and two Ag atoms. However, one-eighth of the rings contain two Sb atoms and one Ag atom, resulting in a stoichiometry of  $[\text{Ag}_5\text{Sb}_3\text{S}_8]^{2-}$  for each honeycomb sheet.

Sulfur atoms within a sheet adopt an approximately close-packed arrangement, and the stacking of a pair of  $[\text{Ag}_5\text{Sb}_3\text{S}_8]^{2-}$  sheets along [001] produces an AB stacking sequence of sulfur atoms. Linkage of two crystallographically distinct sheets by Ag–Sb bonds and by the remaining vertexes of the  $\text{AgS}_4$  (Ag(1), Ag(3), and Ag(4)) tetrahedra produces a buckled double layer of stoichiometry  $[\text{Ag}_5\text{Sb}_3\text{S}_8]^{2-}$  (Figure 5). Ethylenediamine template molecules are located in pairs, held together by relatively strong hydrogen bonding ( $\text{N}\cdots\text{N} = 2.40\text{--}2.63$  Å), in the space between successive double layers, which are separated by ca. 6 Å (Figure 6). The C–C bonds in the template molecules are directed approximately along the [1 0 –1] direction, at an angle of ca. 45° to the  $[\text{Ag}_5\text{Sb}_3\text{S}_8]^{2-}$  layers. Charge-balancing requires monoprotonation of each of the amines, although hydrogen atoms cannot be located directly. Each nitrogen atom is disordered over two crystallographic positions, and all have sulfur neighbors within hydrogen-bonding distance (3.20–3.65 Å), suggesting the presence of hydrogen bonding between the ethylenediamine molecules and the framework.

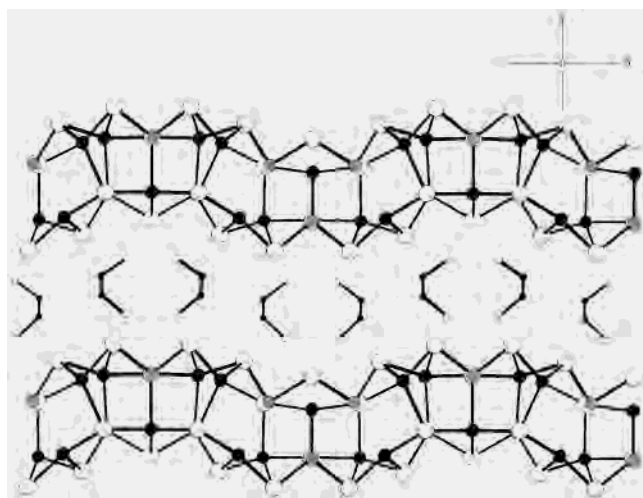


**Figure 6.** View along the [100] direction, illustrating the buckling of the  $[\text{Ag}_5\text{Sb}_3\text{S}_8]^{2-}$  double layers and showing the location of ethylenediamine template molecules in the interlayer space. Only one of the two sites over which nitrogen atoms are disordered is shown. Key as for Figure 3.

The structure of the  $[\text{Ag}_5\text{Sb}_3\text{S}_8]^{2-}$  double layer is unique. However, it may be compared with the double layers in  $[\text{Mn}(\text{en})_3][\text{Ag}_6\text{Sn}_2\text{Te}_8]$ .<sup>30</sup> The latter can be considered as being derived from the antifluorite structure by excision of a block, two anion layers thick, parallel to the (111) crystallographic plane, giving an AB pair of close-packed anion layers with all interstitial tetrahedral sites occupied by cations (Figure 7a).  $[\text{Ag}_6\text{Sn}_2\text{Te}_8]^{2-}$  exhibits a double layer comprised of edge-sharing  $\text{AgTe}_4$  and  $\text{SnTe}_4$  tetrahedra, but the honeycomb-like array possesses a two-dimensional superstructure as the result of cation ordering (Figure 7b). Discrete  $[\text{Mn}(\text{en})_3]^{2+}$  cations separate the  $[\text{Ag}_6\text{Sn}_2\text{Te}_8]^{2-}$  double layers. Along the *c*-axis, the anion layers follow the stacking sequence AB\*BC\*CA, where an asterisk indicates the presence of  $[\text{Mn}(\text{en})_3]^{2+}$  cations. The idealized structure of  $[\text{Ag}_5\text{Sb}_3\text{S}_8]^{2-}$  also comprises two close-packed anion layers in an AB stacking sequence. However, in contrast with the complete occupancy of tetrahedral sites found in  $[\text{Ag}_6\text{Sn}_2\text{Te}_8]^{2-}$ , only half the tetrahedral sites are occupied by cations, the remainder of them occupying all of the available octahedral positions (Figure 7c). The half-occupancy of tetrahedral sites in  $[\text{Ag}_5\text{Sb}_3\text{S}_8]^{2-}$  occurs in an ordered fashion, such that only one type ( $\text{T}^+$  or  $\text{T}^-$ ) is occupied. Distortion of the idealized structure produces buckling of the anionic layers, leading to an effective trigonal pyramidal coordination of Sb and Ag at the “octahedral” interstitial positions. The idealized structure is therefore related to the well-known binary structure of  $\text{Li}_3\text{Bi}$ , of which it may be considered to be an ordered defect variant. Indeed, the simultaneous occupation of half of the tetrahedral and all of the octahedral interstitial sites between pairs of close-packed anion layers has not previously been reported: this therefore represents a new type of solid-state structure.

(30) Chen, A.; Wang, R.-J.; Li, J. *Chem. Mater.* **2000**, *12*, 762.

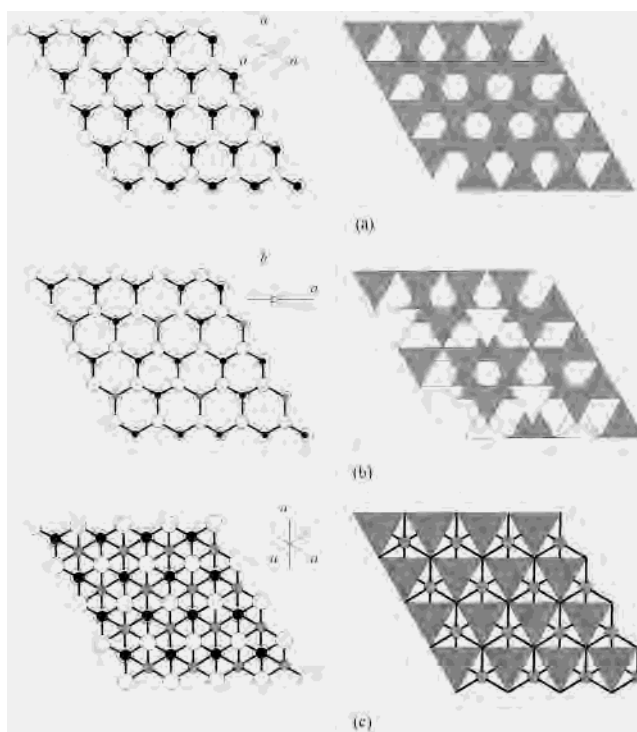


**Figure 7.** Ball and stick (left) and polyhedral (right) representations illustrating the relationship among (a) a block of the antifluorite structure, two anion layers thick, cut parallel to the (111) crystallographic plane, in which all interstitial tetrahedral sites between an AB pair of close-packed anion layers are occupied by cations (cations, black circles; anions, open circles), (b) the double layer of  $[\text{Ag}_6\text{Sn}_2\text{Te}_8]^{2-}$  showing the same structural block as in (a), with a two-dimensional superstructure resulting from ordering of Ag and Sn cations (silver, black circles; tellurium, open circles; tin, shaded circles; in the polyhedral representation, tin, open tetrahedra; silver, shaded tetrahedra), and (c) the idealized structure of a  $[\text{Ag}_5\text{Sb}_3\text{S}_8]^{2-}$  double layer in which half of the interstitial cations are displaced from tetrahedral to octahedral positions (tetrahedral sites, black circles; sulfur, open circles; octahedral sites, shaded circles).

The honeycomb-like array of atoms in the sheets from which **2** is derived comprise fused six-membered rings, in which metal and sulfur atoms alternate. For rings containing two metals, A and B, there are only two possibilities,  $\text{AB}_2\text{S}_3$  and  $\text{A}_2\text{BS}_3$ . The overall stoichiometry of **2** corresponds to sheets containing fused  $\text{AgSb}_2\text{S}_3$  and  $\text{Ag}_2\text{SbS}_3$  rings in a ratio of 1:7. This suggests that there may exist a series of structurally related materials,  $[\text{AgSb}_2\text{S}_3]_x^+[\text{Ag}_2\text{SbS}_3]_y^-$  ( $x \leq y$ ;  $1 \leq y/x \leq 7$ ), containing a varying ratio of the two types of rings and including the neutral sheet  $\text{AgSbS}_2$ . Our current synthetic efforts are directed at exploring such a series.

**Acknowledgment.** A.V.P. thanks The Royal Society of Edinburgh for a research fellowship.

**Supporting Information Available:** CIFs and listings of crystallographic data, atomic coordinates, bond distances and angles, and anisotropic thermal parameters for **1** and **2**. This material is available free of charge via the Internet at <http://pubs.acs.org>.

IC034926U